

# BEAM DYNAMICS IN LANSCE ACCELERATOR FACILITY WITH LOWER ENERGY\*

Y. K. Batygin<sup>†</sup>, E. Henestroza, S. S. Kurennoy, LANL, Los Alamos, NM, USA

## Abstract

In operation of the LANSCE accelerator facility, occasionally it is required to provide beam at a lower beam energy than the nominal energy of 800 MeV. In this paper we examine the regime when the last sector of the LANSCE linear accelerator is off, so that the beam energy becomes 700 MeV. The purpose of our study is to evaluate beam quality and required changes in the accelerator setup. Lower beam dynamics affects Coupled-Cavity Linac, Switchyard, high-energy beamlines, and beam accumulation in Proton Storage Ring (PSR). The original design of the injection beamline to the PSR at a nominal energy of 800 MeV assumes elimination of cross-terms in the beam 6D sigma-matrix at the point of injection. However, these terms are amplified when a 700-MeV beam is injected. Comparison of beam dynamics with nominal and lower energy operation is presented.

## INTRODUCTION

Los Alamos Neutron Science Center (LANSCE) accelerator facility has been in operation for more than 50 years delivering important information for national security and fundamental nuclear physics. Currently it works in multi-beam operation regime, delivering beams to five experimental areas [1]. The layout of the accelerator facility is shown schematically in Figure 1.

The accelerator is equipped with two independent injectors for H<sup>+</sup> and H<sup>-</sup> beams. Each injector has a Cockcroft-Walton type generator and an ion source to produce either positively charged protons (H<sup>+</sup>) or negatively charged hydrogen ions (H<sup>-</sup>) with a final energy of 750 keV. Two independent beamlines deliver H<sup>+</sup> and H<sup>-</sup> beams, merging at the entrance of a 201.25 MHz Drift Tube Linac (DTL). The DTL performs acceleration up to the energy of 100 MeV. After the DTL, the Transition Region beamline directs the 100 MeV proton beam to the Isotope Production Facility (IPF), while H<sup>-</sup> beam is accelerated up to the final energy of 800 MeV in an 805 MHz Coupled Cavity Linac (CCL). The H<sup>-</sup> beams, created with different time structures imparted by a low-energy chopper, are distributed in the Switch Yard to Lujan Neutron Science Center, Weapons Neutron Research Facility (WNR), Proton Radiography Facility (pRad), and Ultra-Cold Neutron Facility (UCN). The accelerator operates at a 120 Hz repetition rate with 625  $\mu$ s pulse length. Parameters of all beams are presented in Table 1.

Within operation, sporadically it is necessary to deliver beams to experimental targets with lower energy. In this paper, we provide initial results of beam dynamics study in accelerator facility with reduced energy.

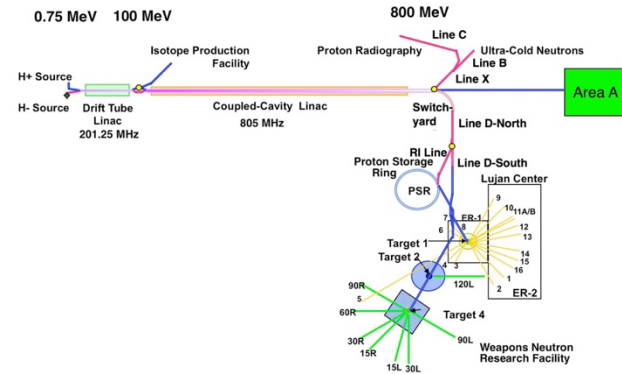


Figure 1: Overview of the LANSCE accelerator and user facility complex.

Table 1: Beam Parameters of LANSCE Accelerator

Area	Rep. Rate (Hz)	Current/Bunch (mA)	Average Current ( $\mu$ A)	Average Power (kW)
Lujan	20	10	100	80
IPF	100	4	230	23
WNR	100	25	4.5	3.6
pRad	1	10	<1	<1
UCN	20	10	10	8

## BEAM DYNAMICS IN COUPLED CAVITY LINEAR ACCELERATOR

LANSCE 805 MHz Side-Coupled Linac (CCL), accelerates particles from 100 MeV to 800 MeV. The CCL consists of 104 tanks, which are grouped into 44 accelerating modules (modules 5-48). Modules 5-12 contain 4 accelerating tanks each, while modules 13-48 contain 2 tanks each. Every tank contains multiple (34 - 61) accelerating cells with constant geometrical velocity within the interval of  $\beta_g = 0.4311 - 0.84056$ . Each CCL module is fed by RF power from a klystron, having a maximum design output power of 1.25 MW with a pulse width of 1000  $\mu$ s. The beam focusing is provided by quadrupole doublets placed between accelerating tanks.

Energy gain per module in CCL is changing from 13 MeV at the beginning of the linac to 16 MeV at the end of linac. The CCL linac has a length  $\sim 700$  m with an average real estate gradient of  $dW/dz = 1$  MeV/m, and average accelerating field  $E = 1.15$  MV/m, providing acceleration with the synchronous phase  $\varphi_s = -30^\circ$ . The transverse CCL normalized acceptance is changing from  $\varepsilon_{ch}$  (100 MeV) =

\* Work supported by US DOE under contract 89233218CNA000001

<sup>†</sup> batygin@lanl.gov

$1.75 \pi \text{ cm mrad}$  at the beginning to  $\varepsilon_{ch}$  (800 MeV) =  $3.5 \pi \text{ cm mrad}$  at the end of machine [2]. The transverse matched Twiss parameters at the entrance to the first CCL tank are  $\alpha_x = 1.228$ ,  $\beta_x = 5.54 \text{ m}$ ,  $\alpha_y = 0.335$ ,  $\beta_y = 3.24 \text{ m}$ .

The longitudinal normalized acceptance is changing from  $\varepsilon_{acc}(100 \text{ MeV}) = 7.46 \pi \text{ cm mrad}$  to  $\varepsilon_{acc}(800 \text{ MeV}) = 25 \pi \text{ cm mrad}$  [2]. The matched beam at the beginning of linac with rms longitudinal normalized beam emittance  $\varepsilon_{z_rms} = 0.175 \pi \text{ cm mrad}$  has size  $R_z = 5.9 \text{ mm}$  and half-momentum spread  $p_\zeta/mc = 1.26 \cdot 10^{-3}$ . Space charge depression parameters of transverse and longitudinal oscillations are  $\mu_t/\mu_s = 0.8$ ,  $\mu_z/\mu_{zo} = 0.9$ , correspondingly, and weakly affect zero-intensity matching parameters.

Simulations of beam dynamics with nominal 800 MeV and lower 700 MeV beam energy were performed with PIC code BEAMPATH [3]. The beam in both cases was selected to be matched with the CCL linac at the initial energy of 100 MeV. The operation regime of lower energy of 700 MeV assumed that the last sector of LANSCE linac, which contains 6 accelerating modules 43-48, was off. It corresponds to turning off last 12 accelerating tanks. In this case, the beam drifted last 102 m, while transverse focusing was kept the same as that for nominal 800 MeV operation. In operation of LANSCE linac, the gradients in quadrupoles in modules 16-48 within energy interval of 260 MeV – 800 MeV are held at the same level of  $\pm 30 \text{ T/m}$ .

Results of simulations are presented in Fig. 2, Fig. 3, Fig. 4, and Table 2. As seen, the normalized beam emittances (both transverse and longitudinal) are almost the same, while the transverse Twiss parameters are changing insignificantly. The most substantial change is the longitudinal beam size at the end of linac, which is transformed from  $10^\circ$  at 800 MeV to  $80^\circ$  at 750 MeV in 805 MHz scale due to long drift of 700 MeV beam without longitudinal focusing. The beam size at the end of linac could be restored via turning on one of the intermediate accelerating tanks, for example, that in module 46 to provide beam bunching (see Fig. 4).

## HIGH-ENERGY BEAM TRANSPORT AT REDUCED ENERGY

After the linear accelerator, the beams are separated in the Switchyard and transported to experimental areas. Currently, there is only  $\text{H}^-$  beam, prepared with various time structures, is distributed between four high-energy targets. The Line D North (LDN) beamline bends the beam to the south end of the accelerator facility. After Line D North, the  $\text{H}^-$  beam is bent by the pulsed kicker magnet RIKI toward the Proton Storage Ring Injection (RI) beamline. Unaffected part of  $\text{H}^-$  beam is directed to the Weapons Neutron Research facility. The RI beamline includes section of decoupling of transverse phase spaces downstream of the achromatic skew bend to avoid dispersion-related beam emittance growth. After RI beamline, the  $\text{H}^-$  beam is injected into Proton Storage Ring through stripping foil,

transforming negatively charged hydrogen ions into protons.

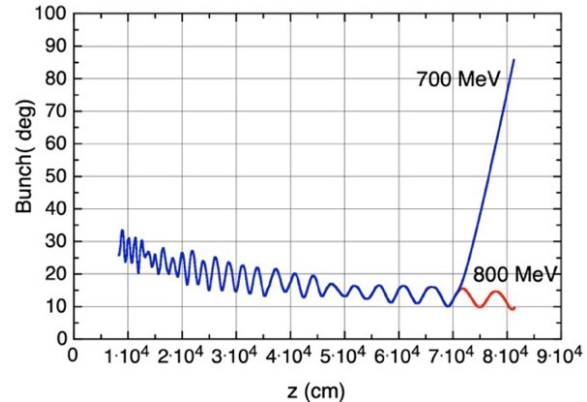


Figure 2: Bunch length (805 MHz scale): (red) all modules ON, (blue) modules 5-42 ON, modules 43-48 OFF.

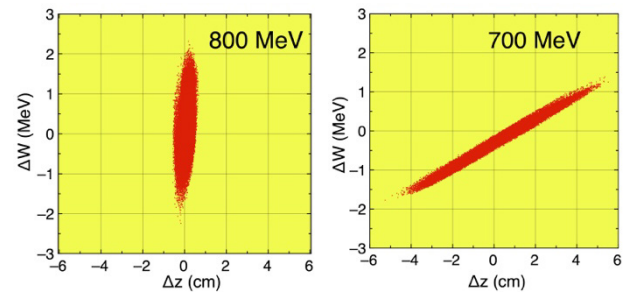


Figure 3: Longitudinal beam phase space after linac: (a) 800 MeV, (b) 700 MeV.

Table 2: Transverse Twiss Parameters and RMS Normalized Beam Emittances ( $\pi \text{ mm mrad}$ ) after Linac

Energy (MeV)	$\alpha_x$	$\beta_x$	$\alpha_y$	$\beta_y$	$\varepsilon_{x_rms}$	$\varepsilon_{y_rms}$
800	0.011	1.22	-0.42	1.53	0.622	0.626
700	-0.32	1.07	-0.76	1.43	0.625	0.627

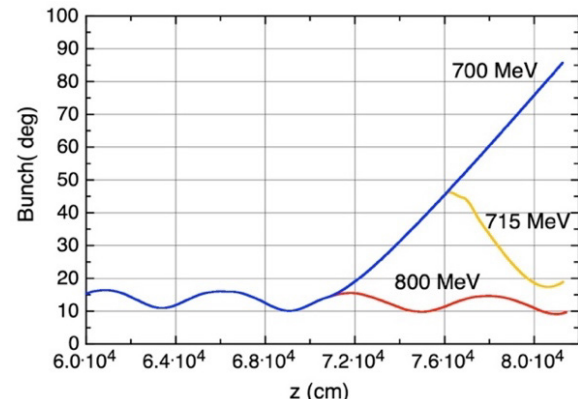


Figure 4: Bunch length (805 MHz scale): (red) all modules ON, (blue) modules 5-42 ON, modules 43-48 OFF, (yellow) modules 5-42 ON, modules 43, 44, 45, 47, 48 OFF, module 46 ON.

Simulations of beam dynamics in a LDN/RI high-energy beamline for nominal 800 MeV and lower 700 MeV beam energy were performed with the Elegant code [4] (see Figs. 5 and 6). In case of 700 MeV beam transport, the values of fields in bending magnets and that in quadrupoles were scaled proportional to particle momentum with a scaling factor

$$u = \frac{(\beta\gamma)_{700}}{(\beta\gamma)_{800}} = 0.9177. \quad (1)$$

Calculations indicate that transverse beam sizes along the high-energy beam transport are almost identical in both cases (see Fig. 5). Simulations confirm that at the energy of 800 MeV, there is no coupling of the beam second-order moments at the foil position, in agreement with the design. However, at the beam energy of 700 MeV, the coupling between the off-diagonal sigma-matrix beam matrix becomes noticeable (see Fig. 6). The largest coupling at the foil position is between the horizontal coordinate and the bunch length.

## BEAM ACCUMULATION IN PROTON STORAGE RING

The LANSCE Proton Storage Ring is the 90.2-m circumference storage ring, accumulating  $\sim 5 \mu\text{C}$  of protons within 625  $\mu\text{s}$  and extracting it to the 1L target within 290 ns. PSR operates at a repetition rate of 20 Hz with 10 mA/bunch  $\text{H}^+$  peak current delivered from linac, corresponding to an average beam current of 100  $\mu\text{A}$  and an average beam power of 80 kW. This beam is chopped before linac within a time interval of 290 ns every 358 ns, which is the revolution time for the Proton Storage Ring at an energy of 800 MeV. After accumulation, the beam is extracted to the moderated neutron spallation target at the Lujan Center. The 68-ns gap allows for the extraction and injection of the beam.

Important aspect in changing of operation regime of Proton Storage Ring is prevention of elevated beam loss. Typical average beam losses in PSR are at the level of 0.25% [5]. The main sources of beam loss are related to stored beam scattering in the stripping foil ( $\sim 0.19\%$  of loss) and delayed stripping of excited states of  $\text{H}^0$  produced in the stripping process ( $\sim 0.04\%$  loss). Additional 0.02% loss are due to beam extraction from PSR. Sources and optimization of beam loss in PSR are discussed in detail in Ref. [5].

With a change of operation energy, all magnet parameters are scaling by a ratio of particle momentum of  $u = 0.9177$ . The characteristic functions as the beta-function, dispersion function, and phase advances of transverse oscillations, remain the same. The PSR revolution frequency is changed from nominal value of  $f_0 = 2.792424 \text{ MHz}$  to new value

$$f = f_0 \frac{\beta_{700}}{\beta_{800}} = 0.9738 f_0 = 2.7192 \text{ MHz}, \quad (2)$$

which corresponds to revolution period of 368 ns. The number of accumulations turns drops from  $\sim 1750$  to  $\sim 1700$ .

The nominal values of incoherent space charge tune shifts at the energy of 800 MeV and beam intensity 70  $\mu\text{A}$  are estimated as  $\Delta\nu_x = -0.22$ ,  $\Delta\nu_y = -0.158$ , while ACCSIM simulations provided smaller values  $\Delta\nu_x = -0.158$ ,  $\Delta\nu_y = -0.125$  [5]. With a decrease in energy from 800 MeV to 700 MeV, the increase in incoherent tune shift,  $\Delta\nu \sim \beta^{-2} \gamma^{-3}$ , is expected to be by a factor of 1.25. However, the space charge effects are not a significant source of beam losses in PSR until the accumulated charge does not exceed 6  $\mu\text{C}$  [5].

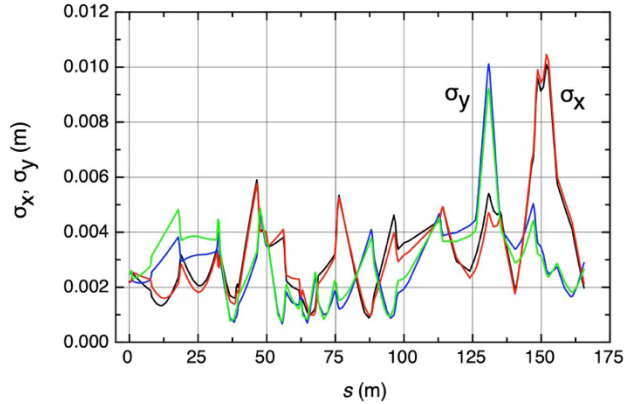


Figure 5: Evolution of transverse beam sizes along high-energy beam transport: (black)  $\sigma_x$ , 800 MeV; (blue)  $\sigma_y$ , 800 MeV; (red)  $\sigma_x$ , 700 MeV; (green)  $\sigma_y$ , 700 MeV.

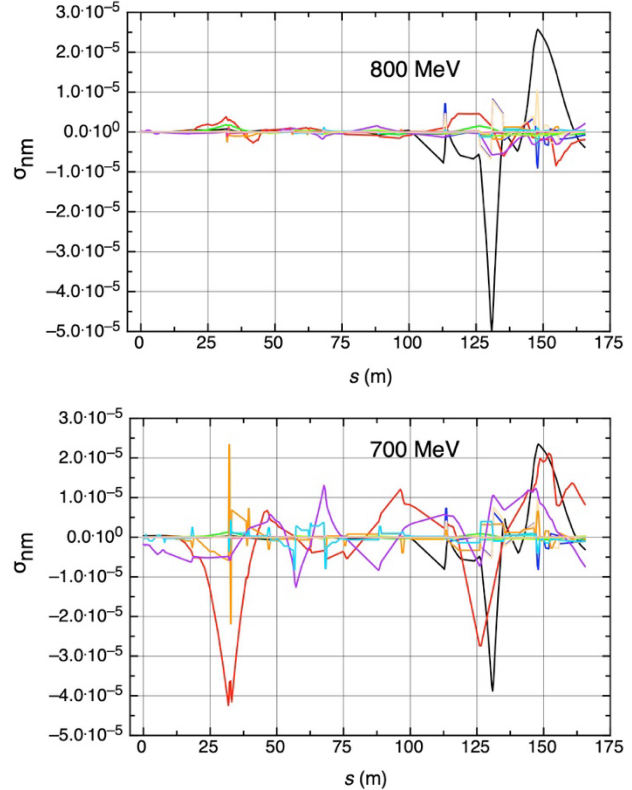


Figure 6: Evolution of off-block-diagonal sigma - matrix elements along high-energy beam transport.

## REFERENCES

- [1] K. W. Jones and P. W. Lisowski, "LANSCE high power operation and maintenance experience", in *Proc. of AccApp'03*, San Antonio, TX, USA, Jun. 2003, p. 372.
- [2] T. F. Fronk, "Aspects of beam stability of the LANSCE accelerator facility", M. Sci. Thesis, Indiana University, Bloomington, IN, USA, 2018.
- [3] Y. K. Batygin, "Particle-in-cell code BEAMPATH for beam dynamics simulations in linear accelerators and beamlines", *Nucl. Instrum. Methods Phys. Res., Sect. A*, vol. 539, pp. 455-489, 2005. doi: 10.1016/j.nima.2004.10.029
- [4] M. Borland *et al.*, "Recent progress and plans for the code Elegant", in *Proc. ICAP'09*, San Francisco, CA, USA, Aug.-Sep. 2009, WE3IOPK02, pp. 111-116.
- [5] R. J. Macek, "PSR experience with beam losses, instabilities and space charge effects," in *AIP Conference Proceedings*, 1998, pp. 116-127. doi:10.1063/1.56765